THE ROLE OF HEMOZOIN IN DISEASE:

OXIDATIVE STRESS

By

Vanessa Jean Scott

Thesis

Submitted to the Faculty of the

Graduate School of Vanderbilt University

in partial fulfillment of the requirements

for the degree of

MASTER OF SCIENCE

in

Chemistry

December, 2009

Nashville, Tennessee

Approved:

Professor David W. Wright

Professor John A. McLean

TABLE OF CONTENTS

Page

LIST OF FIGURES iii

Chapter

I. HEMOZOIN IN SCHISTOSOMIASIS 1
Introduction 1
Lifecycle of *Schistosoma mansoni* 2
Hemoglobin Catabolism and Hemozoin Formation 4
Structure of Hemozoin 6
Beta Hematin 6
Immune Response to Schistosomiasis 7
Aims 8

II. *SCHISTOSOMA MANSONI* INFECTION IN A MURINE MODEL 9
Introduction 9
Experimental 10
Results and Discussion 12
Time study of course of infection in murine model 12
Isolation and characterization of hemozoin from host tissues 13
Conclusions 16

III. DEMONSTRATION OF OXIDATIVE STRESS 17
Introduction 17
Experimental 17
Results and Discussion 22
Proposed mechanisms of BH-mediated lipid peroxidation 23
BH-mediated isoketal (IsoK) formation 23
BH-mediated isoprostane (isoP) and isofurane (isoF) production 24
Signs of stress in host tissues 25
Demonstration of HNE in host tissues 27
Conclusions 27

Appendix

A. ALTERNATIVELY ACTIVATED MACROPHAGES (AAM) 28
B. MEASUREMENT OF UREA LEVELS 31
C. PDTC INHBITION OF NO PRODUCTION 32
D. STANDARD FOR QUANTIFYING ISOK 33
E. IMMS ANALYSIS OF HEME COMPOUNDS 35

REFERENCES 37

LIST OF FIGURES

Figure		Page
1.	Distribution of Schistosomiasis infection	1
2.	Human exposure to schistosome-infected water at Lake Taabo	2
3.	Life cycle of *Schistosoma* spp	3
4.	Stacked dimers of HZ	5
5.	Comparison of *S. mansoni* infected hosts and host tissues by weight	13
6.	UV/visible spectrum of hemozoin isolated from host liver	14
7.	Comparison of HZ accumulation in murine host tissues	14
8.	FT-IR spectrum of HZ	14
9.	XRD spectrum of HZ	14
10.	SEM images of HZ	15
11.	IsoK-pyridoxamine-lactam adduct formation	24
12.	Isoprostane and Isofuran isolated from BH reactions	25
13.	Anti-HNE and H&E stains of host livers	26
14.	Anti-HNE and H&E stains of host spleens	26
15.	Arginase pathway	29
16.	PDTC inhibition of NO production	32
17.	BH and hemin chloride ion mobility.	35

CHAPTER I

HEMOZOIN IN SCHISTOSOMIASIS

Introduction

Considered one among a number of neglected tropical diseases, schistosomiasis continues to be one of the most widespread parasitic infections and has considerable economic and public health consequences.[1, 2] Among parasitic diseases, schistosomiasis is second only to malaria when ranked by the number of people it kills or chronically disables and the disruption of socioeconomic development.[2] Figure 1 shows the distribution of schistosomiasis infection. Schistosomiasis is typically seen in areas where clean water is available in short supply, as schistosome contamination requires human and molluskan hosts to regularly occupy the same body of water as in Figure 2. The

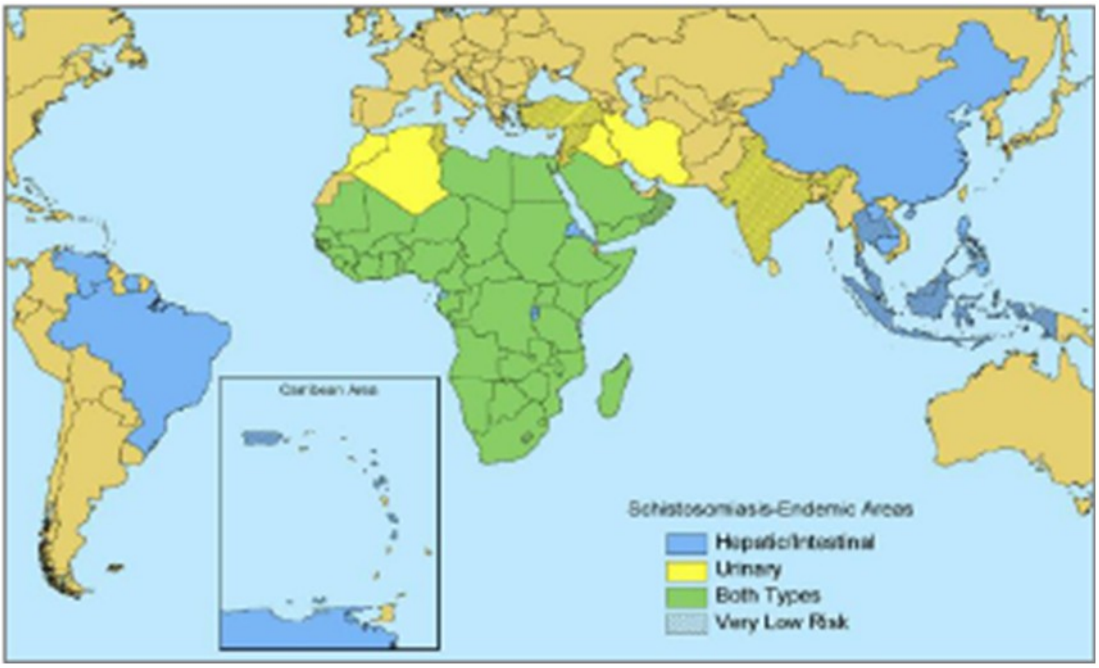

Figure 1. Distribution of Schistosomiasis infection. Schistosomiasis is ranked second only to malaria in parasitic infection and presents over 200 million cases a year with over 200,000 deaths.[3]

Figure 2. Human exposure to schistosome-infected water at Lake Taabo, Cote d'Ivoire.[4]

disease costs an estimated annual loss of about 3.1 million disability adjusted life years.[4] The highest occurrence and infection intensities are seen in school age children, adolescents and young adults, resulting in lowered school perfomance.[5] Schistosomiasis infections undermine social and economic development in strongly afflicted areas.

Lifecycle of *Schistosoma mansoni*

The etiological agent of schistosomiasis, *Schistosoma* spp., maintains a digenetic life cycle. The two hosts, a mammalian species and aquatic mollusks, *Biomphalaria glabrata* for *S. mansoni,* must regularly occupy the same bodies of water. Miracidia search for snails in fresh water and enter the snail through the head or the foot, migrating

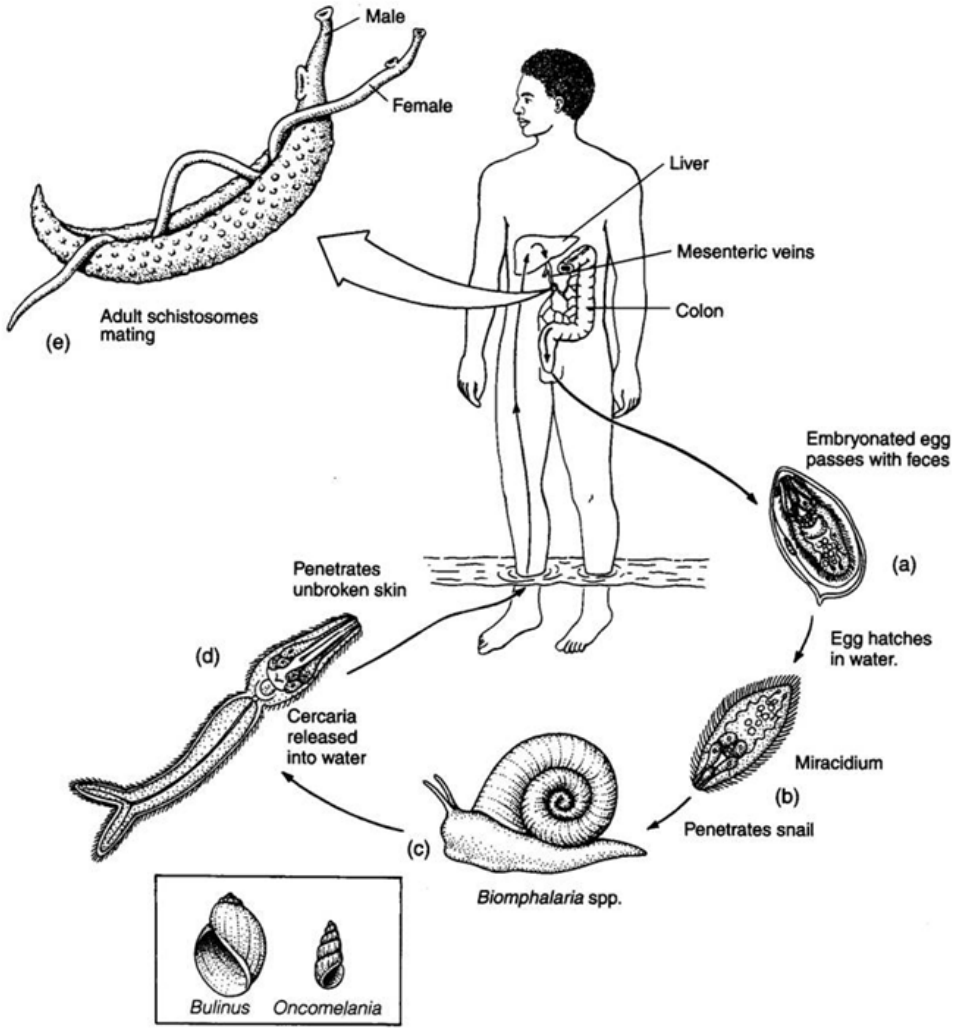

Figure 3. Life cycle of *Schistosoma* spp. *S. mansoni* utilizes the mollusk *Biomphalaria glabrata*; *S. haematobium* uses *Bulinus truncatus truncatus;* and *Oncomelania hupensis hupensis* and *O. hupensis quadrasi* serve as the molluskan host for *S. japonicum*.

to the digestive gland to multiply and develop into cercariae, a process that takes four to six weeks. Cercariae then migrate to the snail's mantle and are shed into fresh water where they seek out mammalian hosts. *B. glabrata* can shed up to 3000 mature cercariae daily from day 28 post exposure for the remainder of the snail's life, and these are viable

in fresh water for up to 48 hours. Cercariae enter their mammalian host through unbroken skin, losing their tails and becoming schistosomulae. The process of host penetration is directed by chemokines and skin surface lipids.[6, 7] Schistosomulae then migrate through the vascular system to mature and take up residence in the hepatic portal vein. Mature blood flukes of *Schistosoma* spp. catabolize host hemoglobin from red blood cells at a rate of about 330,000 red blood cells (RBC) per hour for female worms and 39,000 RBC per hour for males in order to obtain required amino acids.[8] Free heme released in this process is biomineralized to hemozoin (HZ). The stored HZ is visible in the guts of the adult worms. Excess HZ is regurgitated into the host vasculature and engulfed by professional phagocytes. The adult worms pair and lay eggs, up to 300 day per female,[9, 10] and these are either deposited in tissue or shed in feces. About half of the eggs released become lodged in tissue and are responsible for damage done to those tissues. Eggs that are excreted in fresh water release miracidia which then seek out *B. glabrata* to perpetuate the parasites' life cycle. This process is depicted in Figure 3.

Hemoglobin Catabolism and Hemozoin Formation

Hematophagous organisms, which catabolize hemoglobin for amino acids, must evolve a mechanism to contain or detoxify free heme released during this process, as free heme can lead to oxidative stress.[11, 12] The malarial *Plasmodium* spp., kissing bugs of the species *Rhodnius prolixus*, and blood flukes of the genus *Schistosoma* employ a similar solution to this challenge. These organisms sequester free heme, ferriprotoporphyrin IX (Fe(III)PPIX), into a biomineral consisting of centrosymmetric dimers. These dimers form through reciprocal coordination of the propionate side chain of the individual

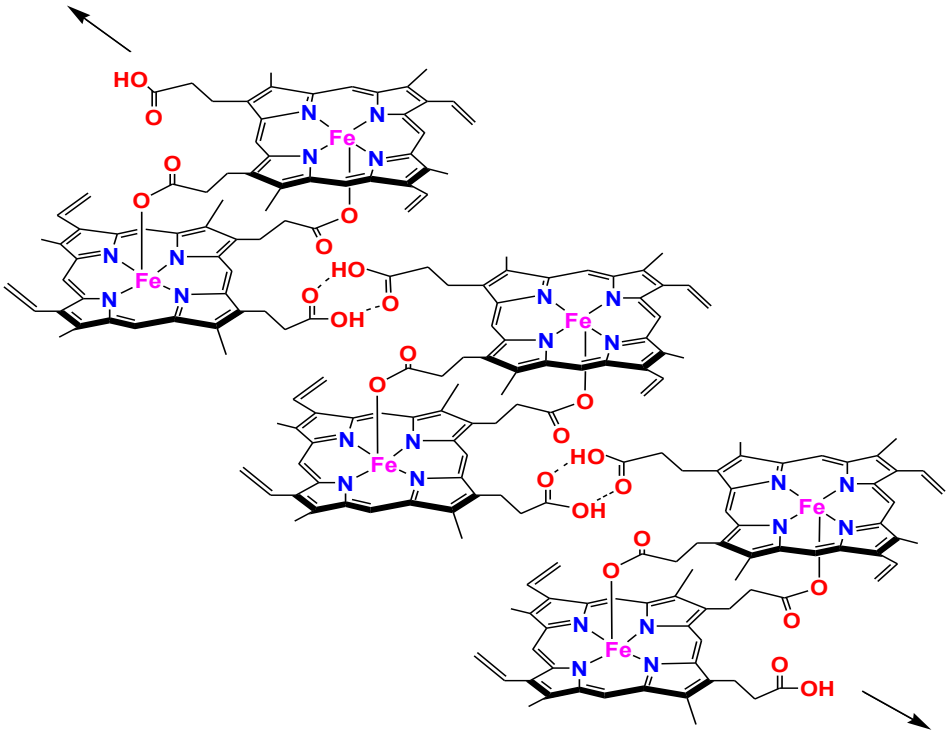

Figure 4. Three stacked dimers of HZ, hydrogen bound through unionized propionic acid side chains. Formation of dimers occurs through Fe–O bonds.

Fe(III)PPIX's to the Fe(III) center of its partner. These dimers then hydrogen bond to other dimers of the same through the unionized propionic acid groups to form a crystal with well defined faces, as shown in Figure 4.[13] This crystalline pigment, observed before the etiological protozoan of malaria itself, came to be known as hemozoin (HZ). Although HZ has been shown to have negative effects both *in vitro* and in cellular systems,[14-23] HZ has been shown to be less toxic to these parasites than free heme due to the reduced availability of the core of the crystal for participation in oxidation-reduction reactioncs.[24] The formation of HZ is therefore a viable method for heme detoxification.

Structure of Hemozoin

The malarial pigment HZ was erroneously described as a hemoprotein until a study by Fitch and Kanjananggulpan in which it was shown by extensive purification to consist of only Fe(III)PPIX.[25] This was confirmed by Slater *et al*. in 1991. Using UV/visible spectroscopy, infrared spectroscopy, and extended x-ray absorption fine structure, Slater *et al*. were able to show that the structure of HZ is identical to that of β-hematin (BH), a synthetic product made from precipitation of Fe(III)PPIX in aqueous solution with acetic acid.[26] This description led to the proposal of a heme polymer, which in turn directed the futile search for a heme polymerase. Six years later, Bohle *et al.* provided further evidence that BH is indeed identical to HZ and suggested a structure of antiparallel polymer chains.[27] Finally in 2000, Pagola *et al*. were able to show that HZ and BH are not polymers, but dimers bound through reciprocal iron-carboxylate linkages of the propionate side chains of each Fe(III)PPIX.[13]

β-Hematin

As native hemozoin (HZ) is available in exceptionally limited quantities and only at a cost of organism life or health, synthetic hemozoin or β-hematin, is utilized in many studies. Crude HZ is defined as pigment that is isolated from parasitized erythrocytes and, although it may be washed to remove cellular debris, the lipid coat adsorbed onto the hydrophobic porphyrin plane is left intact; whereas purified hemozoin is that which has had the lipid coat removed during more intense washing with a detergent or organic solvent.[26, 28, 29] Finally, synthetic hemozoin, BH is synthesized in vitro from hemin chloride and is devoid of all biologically derived components.[22, 30] Characterization of

BH has demonstrated that the material is chemically, spectroscopically, and crystallographically identical to HZ.[13, 25-27]

Immune Response to Schistosomiasis

While the contribution of HZ to pathology in malaria has proposed,[14-17, 20, 22, 31-33] its role in schistosomiasis has been largely overlooked. Studies of pathology in schistosomiasis have concentrated mostly on egg deposition, granuloma formation, and adaptive immune response. The role of HZ in schistosomiasis pathology has been minimally examined. It is the goal of this research to show that HZ has pathological implications in schistosomal infection.

HZ has been shown in malaria to act as a potent immunomodulatory agent. When HZ is phagocytosed by monocytes, these cells become impaired, their ability to accomplish subsequent phagocytic challenges hindered.[14, 15, 20, 34] Phagocytes also have difficulty breaking down HZ; indeed, it can be detected in tissue for at least nine months post parasite clearance.[15, 35] HZ fed monocytes remain viable cells, but become unable to generate oxidative burst with appropriate stimulation[14, 15] and show decreased aptitude for killing ingested microbes.[36] These cells produce less reactive oxygen and nitrogen species, whose purpose is to attack invading particles.[15, 22, 23, 37] HZ has been shown to reduce function of protein kinase C in human monocytes.[16, 17, 32] It has also been shown to affect MHC class II expression[16] and damage dendritic cell function.[38, 39] The presence of HZ has been shown to coincide with products of lipid oxidation.[17, 19, 40]

One of the most examined sources of pathology in schistosomiasis is granuloma formation.[41] A mild type 1 helper T cell (Th1) response occurs in response to adult

parasite antigens. However, when oviposition occurs, this is overshadowed by a vigorous type 2 helper (Th2) response to egg-derived antigen, resulting in fibrogenesis.[42-44] The chronic form of schistosomiasis is characterized by this persistent inflammatory Th2 type reaction leading to granuloma formation.[45, 46] Granulomas form when eggs laid by adult worm pairs get trapped in the microvasculature of the liver. The embryonic miracidium secrete antigens through microscopic pores in the rigid shell of the egg.[47] These egg-derived antigens elicit a response from T helper cells (T_h).[44, 48] Phagocytes attack these egg depositions. These phagocytes are too small to engulf whole schistosome eggs, and usually die trying to attack these eggs. More phagocytes attend the site of infection, and the area around the egg becomes dense with expired immune cells. These granulomas demonstrate inflammation, tissue eosinophilia, and collagen deposition, leading to portal hypertension and severe hepatic fibrosis.[41, 42] Thus, granuloma formation during schistosomiasis is generally looked upon as the fundamental pathological event; however, it has also been shown that granulomas also function to protect tissues from oxidative damage.[49]

Aims

It is the goal of this work to demonstrate that hemozoin contributes to the pathology of Schistosomiasis through the addition of oxidative stress. Chapter II examines the course of the disease using a murine model. Chapter III details products indicative of oxidative stress that can be made *in vitro* in the presence of BH or that have been found in infected tissues.

CHAPTER II

SCHISTOSOMA MANSONI INFECTION IN A MURINE MODEL

Introduction

The murine model offers a uniquely qualified examination of the course of infection of Schistosomiasis and the immune response that is in many ways reflective of these features in human infection. A murine model has been used previously to demonstrate the ability of *S. mansoni* to induce hepatic oxidative stress via the production of reactive oxygen species[50] and reduce antioxidant defense mechanisms of host tissue.[51] Because the course of infection in mice is similar to that in man, it is a useful tool for studying the disease. Thus a time study was embarked upon in order to investigate physiological changes and HZ accumulation over the course of infection by *S. mansoni*.

Native HZ and its synthetic analogue, β-hematin (BH) are identical in structure, but differ dramatically in their availability for collection and surrounding chemical environment. Until recently, the chemical environment of HZ in the parasite and its host remained a mystery largely due to the rigors of extraction and limited sample sizes. Furthermore, BH does not show the same immunomodulatory effects that native HZ does and so, although easier to obtain, is less reliable for HZ host-pathogen studies.[40] Schistosomal HZ has previously been isolated from worms perfused from the hepatic portal vein of host Swiss Webster mice.[52, 53] Methods of isolation of HZ from host liver tissue have been described by Pandey *et. al*.[54] and from host blood by Deegan and Maegraith.[55, 56]

Experimental

Materials

Schistosoma mansoni infected Swiss Webster mice were obtained from the Biomedical research instituted in Rockville, MD. Sodium bicarbonate, monobasic sodium phosphate, dibasic sodium phosphate, sodium hydroxide and dimethyl sulfoxide (DMSO) were obtained from Fisher. Sodium dodecyl sulfate and lipopolysaccharide (LPS) were obtained from Sigma. Anhydrous methyl alcohol, and 2,6-lutidine were obtained from Acros. Dulbecco's phosphate buffered saline (PBS) and RPMI 1640 media with 2 g/L sodium bicarbonate were obtained from Gibco. 4-hydroxy-2-nonenal (HNE) was purchased from Calbiochem. All chemicals were used as received unless otherwise noted.

Time Study

A time study was performed in which 60 Swiss Webster mice were infected by tail exposure to 150 cercariae. Mice were euthanized and examined at 4, 5, 6, 7, and 8 weeks post infection. Control mice were euthanized and examined at the same time as week 8 mice. The adult schistosomes were perfused from the hepatic portal vein, separated by sex and counted. HZ was later extracted from the worms. At the time of perfusion, host spleens and livers were removed, rinsed, weighed, flash frozen in liquid nitrogen and stored at -80°C. Tissues were homogenized and examined for HZ content. Thin tissue sections were stained with hematoxylin and eosin (H&E) and analyzed for lipoxidation products.

Isolation, Characterization, and Measuring of HZ from tissues

HZ was extracted from the livers and spleens collected in the time study. Organs were individually homogenized using Wheaton 15 mL glass homogenizers. The homogenate was rinsed with deionized water into individual 50 mL polypropylene tubes and centrifuged at 1000 x g for 1 minute. The supernatant was removed and centrifuged at 3900 x g for 2 hours. The supernatant was discarded and the pellet rinsed in 1 mL of 150 mM phosphate buffer, pH 7.4 (28.5 mL of 0.2 M monobasic sodium phosphate, $NaH_2PO_4 \bullet H_2O$, with 121.5 mL of 0.2 M dibasic sodium phosphate, $Na_2H_2PO_4 \bullet 7H_2O$, diluted to 200 mL). The pellet was vortexed slightly and light colored tissue was removed along with phosphate buffer. 500 µL of 150 mM phosphate buffer and 500 µL of ethyl acetate were added to the remaining dark pellet. The pellet was vortexed, centrifuged at 1000 x g for 1 min, and the supernatant removed. This last step was repeated until supernatant appeared clear. The alleged HZ pellet was dried under nitrogen gas and confirmed via UV/visible spectroscopy (UV/vis), Fourier-transform infrared spectroscopy (FT-IR), powder x-ray diffraction (XRD) and scanning electron microscopy (SEM).

Dried HZ from host organs was ground using mortar and pestle, mixed with dry KBr and pelleted using a hydraulic press for FT-IR. Dried HZ from host organs was ground using mortar and pestle and analyzed by XRD on a Scintag X1 h/h automated powder diffractometer with a copper target, a Peltier-cooled solid-state detector and a zero-background silica (510) sample support. in a 12 hour run. SEM samples were dissolved in ethanol, dried to SEM mounts, and gold-sputtered for 200 seconds before imaging on a Hitachi S-4200 SEM.

HZ collected from the time study was quantified using a method based on that described by Sullivan.[57] HZ was scraped from 50 mL polypropylene tube into a mortar and pestle where it was ground to a fine powder. The sample was then rinsed back into the same polypropylene tube with 10 mL of 150 mM phosphate buffer, pH 7.4. The mixture was then sonicated and vortexed immediately before pipetting 500 μL of solution into 500 μL of 20 mM NaOH, 2%SDS to dissolve HZ into individual heme units. The mixture was allowed to sit for 1 hour before the absorbance was read at $\lambda = 400$ nm. The resultant concentration of heme was determined using Beer's law and $\varepsilon = 10{,}000$ for heme. This was repeated for 5 livers and spleens from hosts for weeks 4 through 8 of the time study.

Results and Discussion

Time study of course of infection in murine model

Over the eight weeks encompassed by the time study, the livers of infected mice were shown to more than double in size, increasing from 5% of body weight for uninfected mice to more than 15% of total body weight by week 8 of infection. The size of the spleen increased in a similar manner from 0.4% to about 3% of the total body weight. The overall body weight of the infected mice was the same or lower than control mice at eight weeks, indicating that the increased weight of the inflamed organs was accompanied by decreased overall mouse body weight. Worm recovery via perfusion of the hepatic portal vein averaged about 22% of cercarial infection, with a peak worm recovery seen at week six.

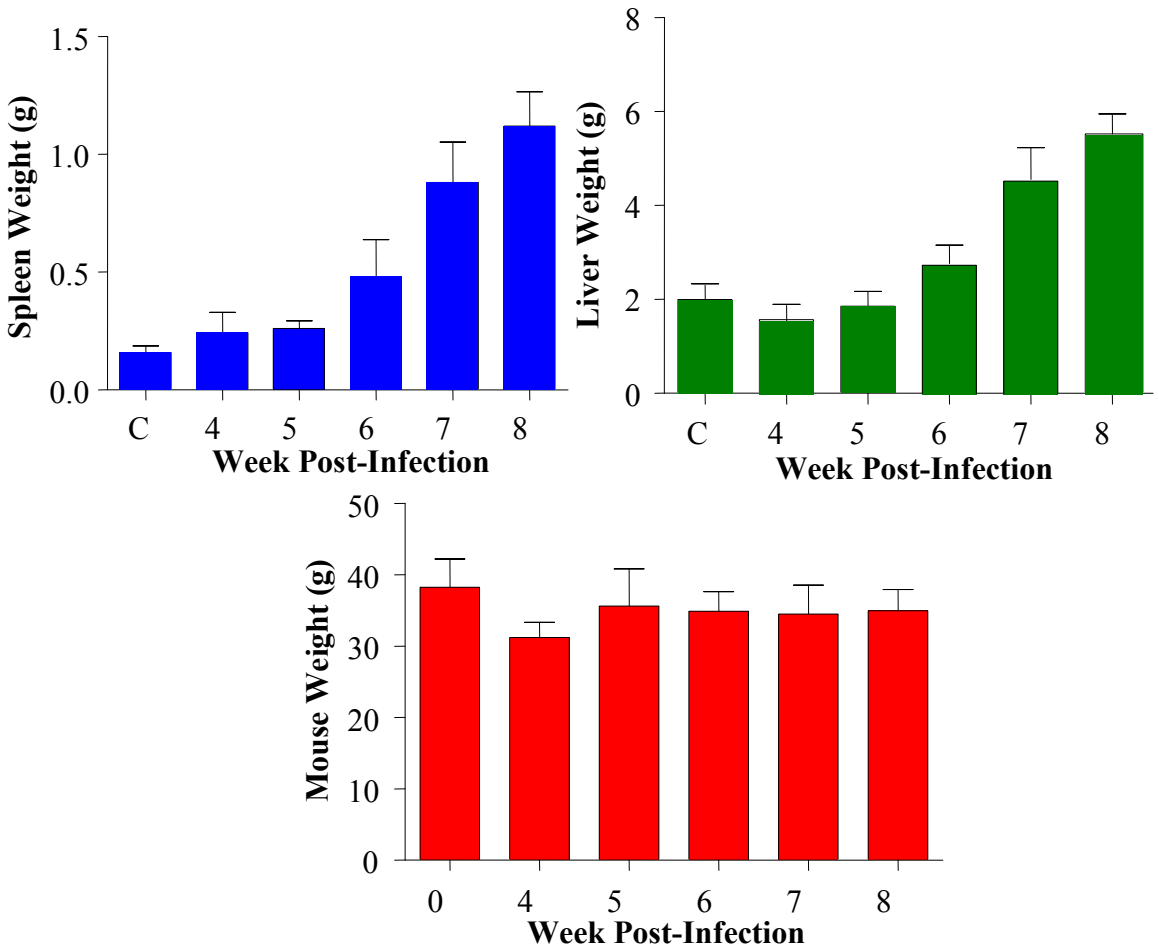

Figure 5. Comparison of *S. mansoni* infected hosts and host tissues by weight over course of infection.

Isolation and characterization of hemozoin from host tissues

Structurally, chemically, and spectroscopically, the HZ isolated from murine tissues appears identical to all previously identified forms, including BH and malarial pigment. The UV/vis spectrum of liver isolated HZ in Figure 6 shows the characteristic Soret band at 400 nm for heme. Average HZ content per organ per week is compared in Figure 7. The FT-IR spectrum, depicted in Figure 8, showed stretches at 1659 cm^{-1} and 1235 cm^{-1}; the accepted values are 1664 and 1211 cm^{-1} for C=O and C—O, respectively. In Figure 8, the liver homogenate hemozoin is shown in blue, BH is shown in red, and

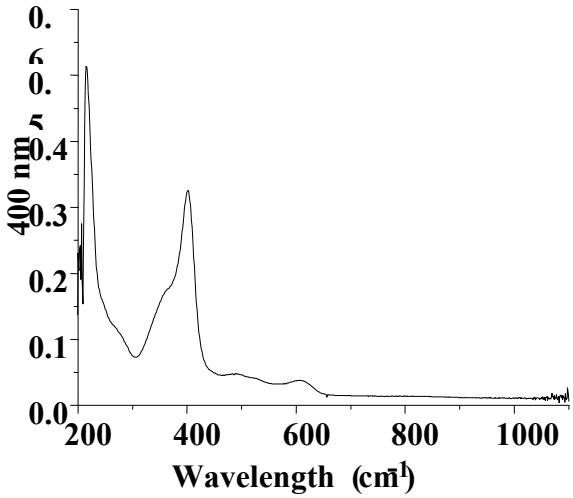

Figure 6. UV/vis spectrum of HZ isolated from *S. mansoni* infected murine liver.

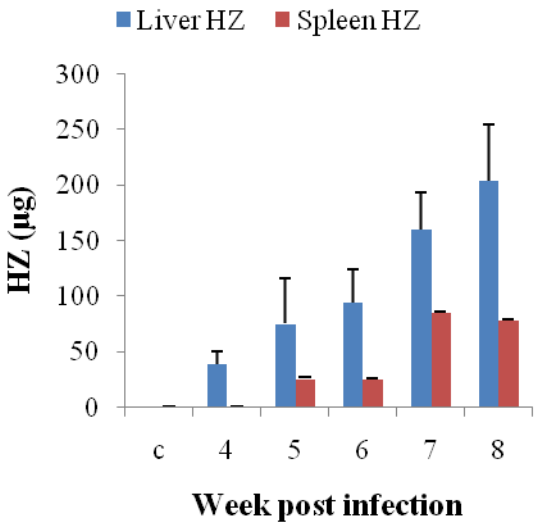

Figure 7. Comparison of HZ accumulation in murine host tissues.

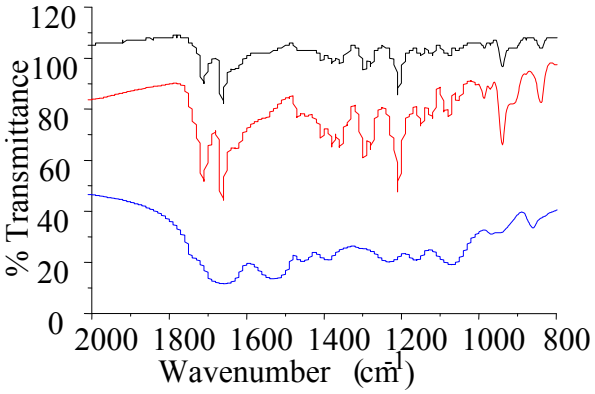

Figure 8. FT-IR spectrum of HZ isolated from *S. mansoni* in black, from infected liver tissue in blue, and from BH in red.

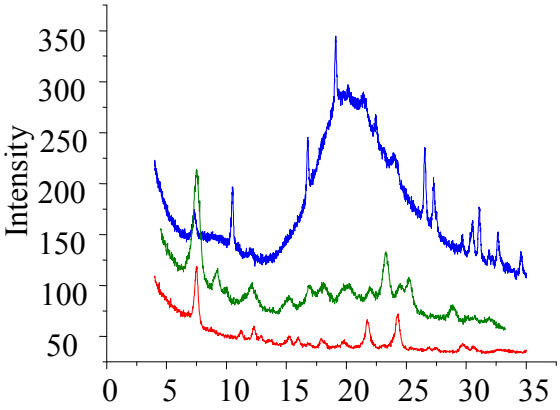

Figure 9. XRD spectrum of BH in red, liver isolated HZ in blue and hemin in green.

HZ isolated from homogenized Schistosomes is shown in black. The expected peaks are present; however, the percent transmittance is much lower in the native hemozoin sample due to a possible lipid coating.

X-ray diffraction of tissue originated HZ showed characteristic 2θ peaks at 7º, 21º, and 24º. Figure 9 shows the XRD pattern of liver HZ in blue, along with hemin in

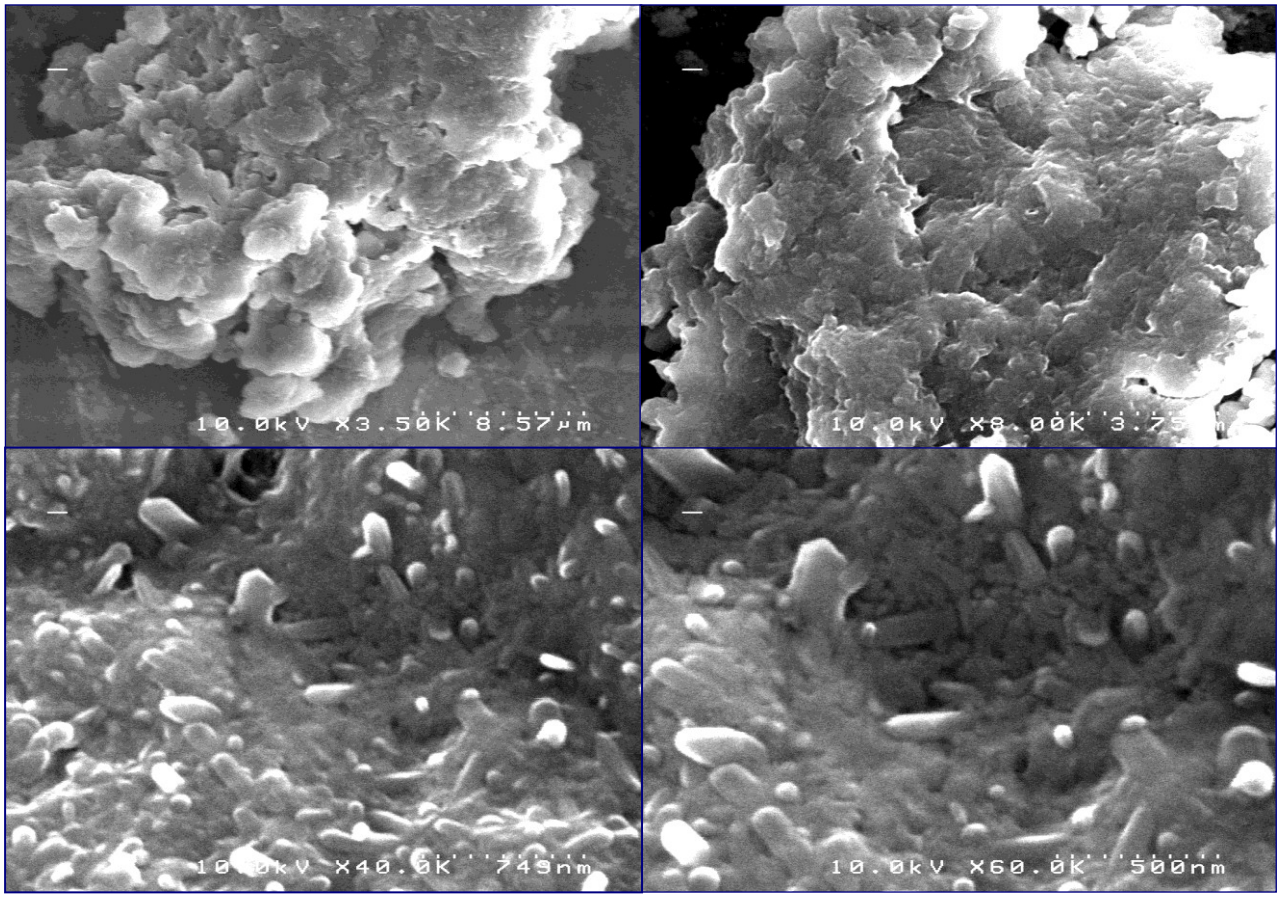

Figure 10. SEM images of HZ isolated from *S. mansoni* infected murine livers. Images shown at 8.57 µm, 3.75µm, 749 nm, and 500 nm.

green and BH in red. The hemin, which is the main substrate for the synthetic BH, shows a peak at 23º that is noticeably absent in the synthetic product and the tissue HZ. The expected peaks for hemozoin are noted in the liver hemozoin pattern; however, additional peaks are also observed as well as an increase in background, likely due to anisotropy in the native sample as compared to the more crystalline synthetic samples.

SEM images of HZ were bright due to remaining sample charge. In general, the sample displayed a large size distribution and heterogeneous morphology, as would be expected from a native hemozoin sample formed along a lipidous template and organized by cellular processing.[52, 58] Figure 10 shows SEM images of hemozoin collected from

host tissue at 8.57 μm, 3.75 μm, 7.49 nm, and 667 nm, respectively. On the nanometer scale, rods of crystalline hemozoin can be observed. Similar rods were noted previously in hemozoin from the malarial parasite *Plasmodium falciparum.*[59]

Conclusions

A new method was developed for the isolation of HZ from murine host tissue. Previous methods for isolation of HZ from host tissues lacked the simplicity of this new method.[54] Yields of HZ from host tissue over the course of an eight week infection were compared, and a steady increase of HZ in tissues was shown, although relative parasite burdens remained relatively constant. This indicates that HZ remains in the tissue rather than being discarded by the host immune system. This has been shown previously in malaria.[15, 35]

CHAPTER III

DEMONSTRATION OF OXIDATIVE STRESS

Introduction

Heme-based compounds are significant sources of non-enzymatic lipid oxidation.[60] The lipoxidation products generated have the ability to modify immune responses. Hemozoin has been shown to modify the biological response of phagocytes that engulf it.[14, 15, 20, 34] Furthermore, the presence of HZ has been shown to coincide with biologically active products of lipid oxidation.[17, 19, 40] In Chapter III, more evidence of HZ as a generator of immunomodulatory oxidation products is offered.

Experimental

Materials

Sodium bicarbonate, monobasic sodium phosphate, dibasic sodium phosphate, dimethyl sulfoxide (DMSO), 2-propanol, and acetic acid were all obtained from Fisher. N-(1-naphyl)ethylenediamine (NED), sulfaniliamide, hemin chloride (bovine), and lipopolysaccharide (LPS) were obtained from Sigma. Anhydrous methyl alcohol, and 2,6-lutidine were obtained from Acros. Arachidonic acid was obtained from Nu-Chek Prep, Inc. Dulbecco's phosphate buffered saline (PBS) and RPMI 1640 media with 2 g/L sodium bicarbonate were obtained from Gibco. RPMI was supplemented with 10% fetal bovine serum (FBS, Atlanta Biologicals) and 100 μg/mL penicillin-streptomycin (P/S, Cellgro Media Tech) before use. 4-hydroxy-2-nonenal (HNE) was purchased from

Calbiochem. HNE immunohistochemical staining reagents were purchased from R&D Systems. Packed red blood cells (RBC) were a donation from the VUMC Blood Bank. All chemicals were used as received unless otherwise noted.

β-Hematin (BH) synthesis and characterization

BH was synthesiszed via a dehdrohalgenation reacton as previously described.[30, 40] Purified hemin chloride (Fluka, 3.0 g) was dissolved in 5 mL of 2,6-lutidine with stirring under an inert atmosphere. Forty mL of 1:1 dimethylsulfoxide (DMSO) /anhydrous methanol was added to the flask with stirring. The flask was sealed, covered in foil, and left undisturbed for ninety days. The solution was then removed from the glove box and crude BH was collected via vacuum filtration with a 0.45 μm filter. BH was washed with methanol (MeOH), DMSO 0.1 M sodium bicarbonate ($NaHCO_3$, pH 9.0), and deionized water. BH purity was monitored with UV-visible spectroscopy established by baseline absorption of the Soret band for heme in the supernatant of the washes. BH was then dried for 48 hours at 150˚C. Product was confirmed by powder X-ray diffraction (XRD), Fourier Transform Infrared Spectroscopy (FT-IR), and scanning electron microscopy (SEM). XRD studies were performed with a Scintag X1 h/h automated powder diffractometer with a copper target, a Peltier-cooled solid-state detector and a zero-background silica (510) sample support. XRD study parameters were as follows: 0.02 step size, 25 second preset time, scan range 4 to 35˚ 2θ. FT-IR spectroscopy was performed on an ATI Mattson Genesis Series FT-IR spectrophotometer using KBr pellets prepared with dried BH. A Hitachi S4200 SEM was used to image BH. BH was suspended in ethanol, sonicated, applied to a polished aluminum specimen

mount, and dried at 25˚ C overnight. The sample was sputter-coated with gold for 20 seconds prior to imaging.

BH-mediated isoketal (IsoK) formation

Arachidonic acid (AA, 10 mM) was oxidized in 1.25 mL of 100 mM phosphate buffer (chelexed, pH 7.4) in the presence of BH at concentrations of 0.48, 0.36, 0.24, 0.12 and 0.00 mM. 250 μL of ethanol was added to the reaction mixture to aid in solublizing AA. The reaction was stirred for two hours at room temperature before 100 μM pyridoxamine dihydrochloride was added. The reaction continued to stir at room temperature for two more hours. Reaction mixtures were extracted with diethyl ether. The organic layers of each sample were combined and dried down. The samples were then redisovled in 50μL of acetonitrile.

Liquid chromatography-tandem mass spectrometry (LC-MS/MS)

LC-MS/MS analysis of isoketal products was performed using a ThermoFinnigan TSQ Quantum triple quadruple equipped with a ThermoFinnigan Surveyor LC. Products were separated on a Magic Bullet C18AQ micro column (3 μm, 100 Å, Michrom BioResources, Auburn, CA) with the gradient programmed from 100% solvent A (5 mM ammonium acetate with 0.1% acetic acid) to 100% solvent B (acetonitrile/methanol 95:5) from 0.5 minutes to 3 minutes and then continuing at 100% B for an additional 1.5 minutes. The column was then equilibrated to 100% A for 2.5 minutes. The flow rate was set to 190 μL/min and the injection volume was 5 μL. The mass spectrometer was operated in positive ion mode with a spray voltage of 3.7 kV, a capillary temperature of

210˚C, a capillary voltage of 35 V, source CID of 5 V, and collision energy of 30 eV. Product scan spectra of the isoketal-pyridoxamine-lactam adduct ([M+H$^+$]) m/z 501 were acquired from 50 m/z to 520 m/z. Selective reaction monitoring (SRM) was used to confirm m/z 501→m/z 152 and m/z 332 transitions, calculated as -17 Da from the parent isoketal-pyridoxamine-lactam mass. Data was acquired and analyzed using Thermo-Finnigan Xcalibur software.

Isoprostanes from BH-mediated ghost membrane peroxidation

RBC ghosts were prepared from expired whole blood obtained from the Vanderbilt Medical Center Blood Bank. Whole blood was kept at 4˚C until use and mixed inside the bag before use. A 22 gauge needle fitted to a disposable syringe was used to draw 3 mL of whole blood which was then expelled into a 15 mL polypropylene centrifuge tube. 11 mL of phosphate buffered saline (PBS) was added and the tube was gently inverted to mix. The solution was then centrifuged on a Beckman Coulter Allegra x-22R centrifuge at 1000 xg for 10 minutes in the Beckman SX4250 swing bucket rotor. The supernatant was discarded in bleach, and this wash was repeated until the supernatant appeared clear. The RBCs were then lysed by dissolving the pellet in 0˚C 5 mM sodium phosphate buffer in 50 mL polypropylene tubes and vortexing. The solution was then centrifuged at 10,000 xg using the fixed angle Beckman C0650 rotor. The supernatant was discarded, and this wash was repeated until no trace of red could be seen in the membrane pellet. The pellet was then dissolved in a minimum amount of PBS and aliquoted to be stored at -80˚C. A Biorad assay was used to determine the protein content of the final solution. Briefly, standards were made with bovine serum albumin from 1.5

mg/mL to 0.2 mg/mL. 5 μL of standards and samples were pippetted into a clean, dry 96 well plate. 25 μL of Bio-rad reagent A, an alkaline copper tartrate solution, were added to each sample followed by 200 μL of reagent B, a dilute 1,2-naphthoquinone-4-sulfonate solution. The plate was allowed to sit for 15 minutes, after which the absorbance was read at 750 nm. RBC ghosts were used for reactions at protein concentrations of 1 mg/mL, as determined by the Biorad Protein assay.

RBC ghosts were stirred in the presence of oxygen with ethanol, 10 mM BH, arachidonic acid, and phosphate buffer quantity sufficient to 800 μL for four hours before the reaction was stopped with 50 μL of 1 M HCl. The samples were then immediately delivered to the lab of L. Jackson Roberts for isoprostane analysis.

Stains of S. mansoni infected murine tissues

Livers and spleens from the time study mentioned above were affixed to glass slides by the Vanderbilt University Immunohistochemistry core. Thin sections were sliced at a thickness of 5 μm. Two stains were made, hematoxylin and eosin (H&E) stains were used to examine cell morphology. 4-hydroxy-2-nonenal (HNE) stains were used to verify the presence of elevated levels of HNE in infected tissue. Staining for 4-hydroxynonenal was done using an anti-HNE monoclonal antibody from R & D Systems and a R & D Systems cell and tissue staining kit. The sample was covered with 2 drops of a 3% peroxide solution to block peroxidase. The reagent did not readily sit on the paraffin sealed tissue section and so was held in place with a glass cover slide. The sample sat in peroxidase blocking reagent for 5 minutes followed by a 5 minute wash with phosphate buffered saline solution (PBS). The slide was then incubated with 2

drops of serum blocking reagent for 15 minutes. The slide was drained, but not rinsed, and then incubated with 2 drops of an avidin solution containing 0.1% sodium azide. The slide was then rinsed with sterile PBS, drained and excess buffer blotted from the sample. The slide was then incubated with 2 drops of a biotin blocking reagent for 15 minutes at room temperature. The slide was then rinsed with buffer and incubated at 37°C with 25 µL of the primary antibody, monoclonal anti-4-hydroxynonenal, at 25 µg/mL for 1 hour. The sample was rinsed with buffer 3 times for 15 minutes each wash. The slide was then incubated with 2 drops of biotinylated secondary antibody for 60 minutes at 37°C. Following another 3 fifteen minute washes with PBS, the slide was incubated with 2 drops of a high sensitivity streptavidin horse radish peroxidase conjugate for 30 minutes at 37°C. After another 3 cycle PBS wash, 2 minute each wash, the slide was then blotted to remove excess buffer. The slide was then treated with 25 µL of a chromogen, a 2% 3-amino-9-ethylcarbazole solution mixed with a 0.1% peroxide solution to activate. The slide was incubated with this chromogen for 1 hour and 20 minutes at 37°C. This process was repeated for livers and spleens collected from the time study for weeks 4, 5, 6, 7, and 8 post infection as well as controls. Images were obtained on an Olympus BH2-RFCA light microscope coupled with and Olympus DP70 camera.

Results and Discussion

This thesis seeks to implement hemozoin as a source of oxidative stress in schistosomiasis. To that effect, the ability of HZ to generate oxidative stress markers *in vitro* was examined. Also the detection of an oxidative stress marker in host tissues coinciding with HZ tissue deposits is disclosed.

Proposed mechanisms of BH-mediated lipid peroxidation

Mechanisms associated with non-enzymatic arachidonic acid peroxidation result in primary hydroperoxide species which differ by the location of that group along the carbon backbone. These are known as n-hydroperoxyeicosatetraenonic acids (n-HPETEs), where the number replacing n identifies the position of the hydroperoxide moiety. These primary peroxidation products are generally short lived and lead to many secondary peroxidation products, including notably isoprostanes, isoketals, and 4-hydroxynonenal, along with many others.

BH-mediated isoketal (IsoK) formation

IsoKs are 1,4-dicarbonyl compounds that are known markers of oxidative stress.[61] They readily adduct to proteins at lysine residues, resulting in pyrrole, lactam, and hydroxylactam adducts. Due to their labile nature, isoKs are short-lived as products. To that effect, the scavenger molecule pyridoxamine was added to these reactions for the purpose of detection via LC-MS/MS. Pyridoxamine has been shown to react quickly and selectively with isoKs.[62] The isoK-pyridoxamine-lactam adduct was observed as a parent 501 m/z with transitions to 152 m/z and 332 m/z products.

Not only was BH able to induce isoK production from arachidonic acid, but also in reactions in which arachidonic acid was stirred in the presence of oxygen with increasing concentrations of BH, relative peak areas were observed to increase with increasing BH concentration, as shown in Figure 11. Attempts to quantitatively study isoK are documented in Appendix D.

BH-mediated production of isoprostanes (isoP) and isofurans (isoF)

Isoprostanes and isofurans have also been shown as indicators of oxidative stress, in malaria and other diseases.[63] In continuing the search for markers of oxidative stress able to be generated by the presence of BH, reactions were arranged in which BH was allowed to stir in the presence of oxygen with RBC membranes and arachidonic acid.

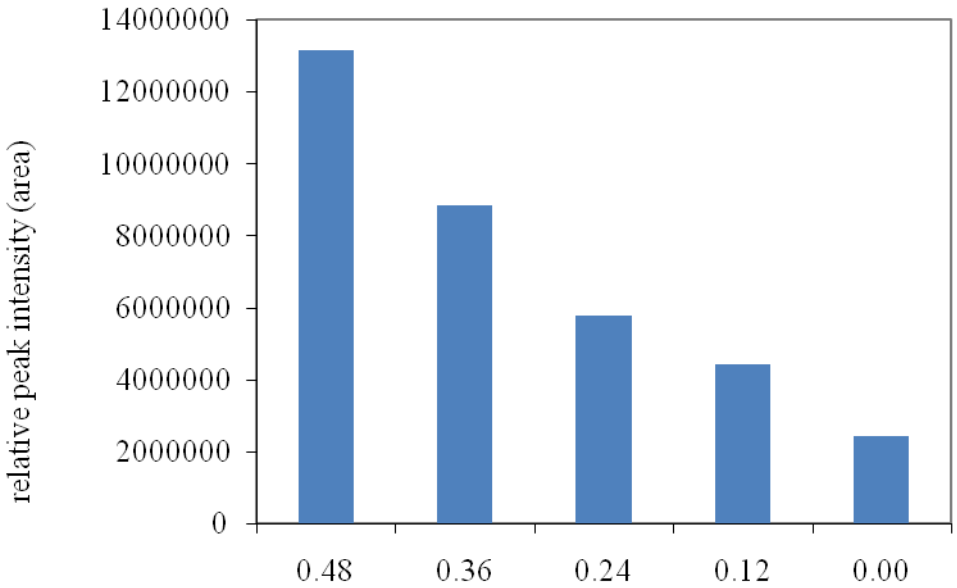

Figure 11. IsoK-pyridoxamine-lactam adduct was detected via LC-MS/MS in extracts from reactions of arachidonic acid and BH, using pyridoxamine as a scavenger. This chart compares the relative amounts detected in reactions with increasing concentrations of BH.

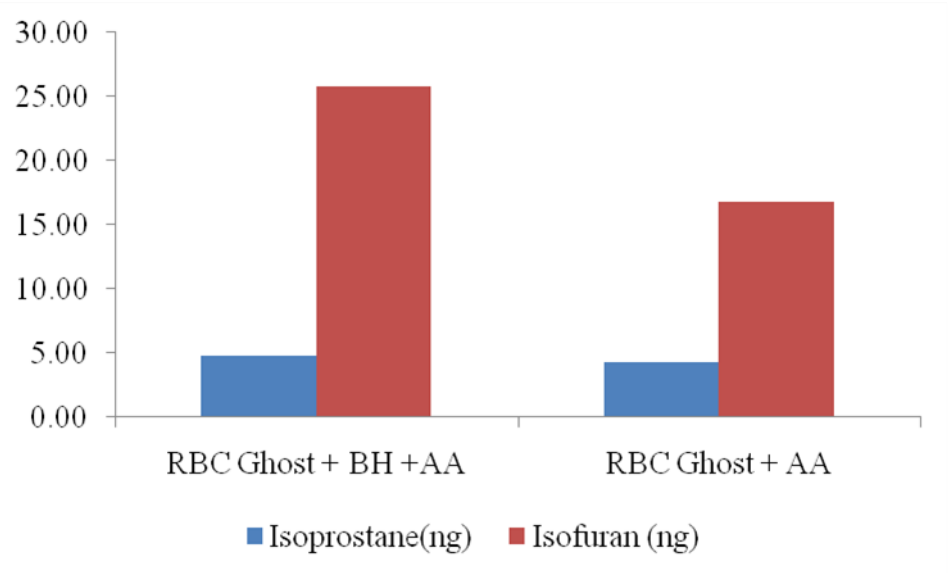

Figure 12. Isoprostane and Isofuran isolated from BH reactions with arachidonic acid and RBC ghosts.

These reactions were stopped and taken to Brooke Gliga in L. Jackson Roberts lab for extraction and determination of isoP and isoF levels. Figure 12 shows her reported levels of isoP and isoF.

Signs of stress in host tissues

Hematoxylin and eosin stains of stains of *S. mansoni* infected mouse liver and spleen thin sections from the time study described above were examined. In these stains, fibrotic granulomas which surrounded the eggs of the parasites were clearly observed in the livers of later weeks of the time study as opposed to controls. Also, in spleen tissue, by week eight post infection, megakaryocytes were observed. Megakaryocytes in the spleen, indicative of extramedullary hematopoiesis, are seen most often as a result of pathologic process and are a sign of stress in an organism.[64] The H & E stains are shown

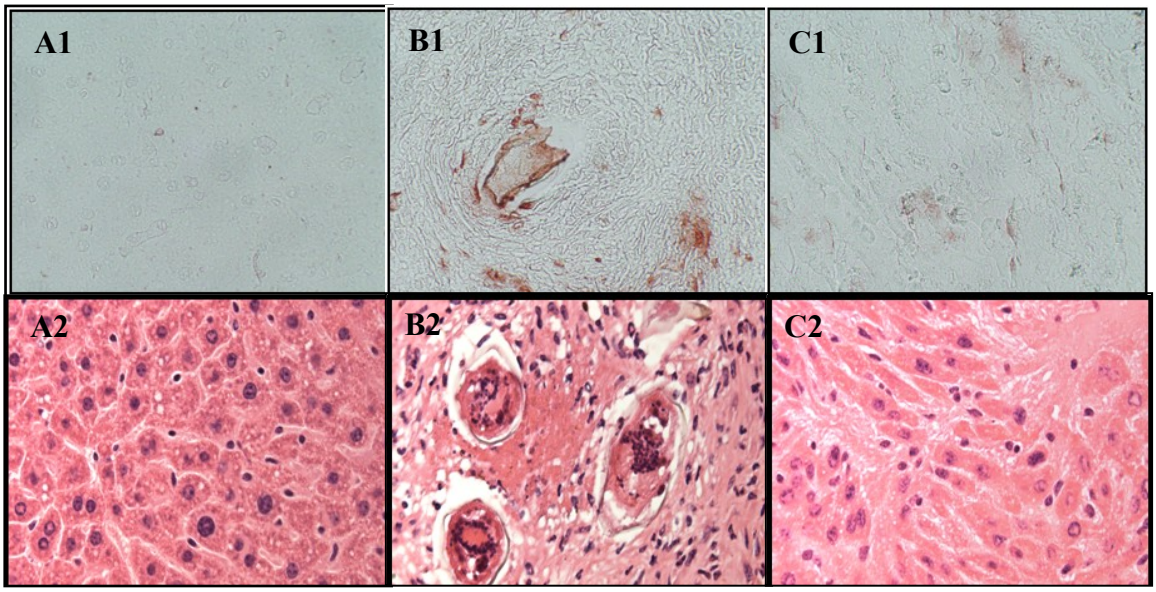

Figure 13. Anti-HNE (1) and H&E (2) stains of uninfected (A) murine livers and murine livers infected by *S. mansoni* at 8 weeks (B) and 4 weeks (C) post infection. All images shown at 40x magnification.

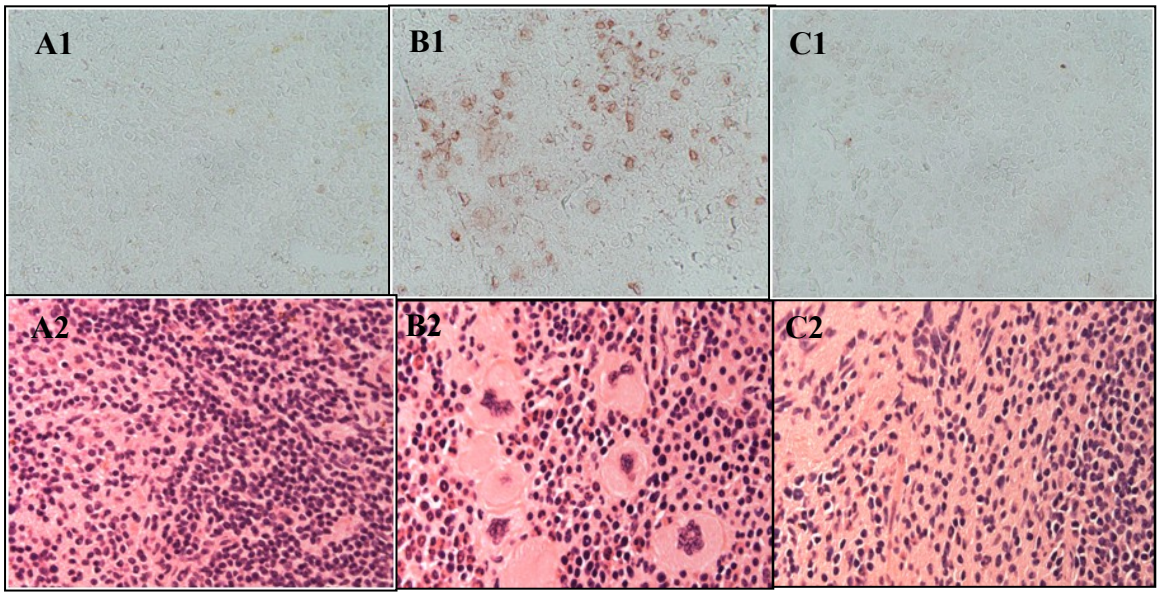

Figure 14. Anti-HNE (1) and H&E (2) stains of uninfected (A) murine spleens and murine spleens infected by *S. mansoni* at 8 weeks (B) and 4 weeks (C) post infection. All images shown at 40x magnification.

alongside HNE immunohistochemical stains for comparison in Figure 13 for livers and Figure 14 for spleens.

Demonstration of HNE in host tissues

4-hydroxynoneal (HNE) is a product of non-enzymatic oxidation of cell membrane components.[65] Immunohistochemical stains for 4-hydoxynonenal were performed on liver and spleen thin sections from mice infected with *S. mansoni*. Concentrated pink to red staining was seen in certain cells of the liver and spleen tissues. The progression of these changes is shown with H&E stains from corresponding weeks for comparison. Figure 13 shows images of liver stains, and Figure 14 shows images of spleen stains.

Conclusions

Given that morbidity and mortality associated with schistosomiasis is associated with liver fibrosis, it should be noted that reactive products of liver peroxidation promote fibrogenesis.[66] The data presented in this chapter entails the production of a few of these peroxidation products, namely isoKs and isoPs, *in vitro* in the presence of BH and shows the coinciding of another oxidative stress marker, HNE in proximity to BH deposits in *S. mansoni* infected tissues.

APPENDIX A

ALTERNATIVELY ACTIVATED MACROPHAGES AS A MODEL FOR SCHISTOSOME-INDUCED IMMUNE RESPONSE

Alternatively activated macrophages (AAMs) were attempted in murine RAW 264.7 cells.[67-69] Activated macrophages are used to study innate immune responses while AAMs provide a model to study humoral immunity including repair processes. Macrophages, which are a major feature of egg-induced granulomas, possess two enzymes, nitric oxide syntase-2 (NOS-2) and arginase-I (Arg-I) that compete for a single substrate, L-arginine. NOS-2 transforms L-arginine to nitric oxide and L-hydroxyarginine, which can inhibit Arg-I. This is part of the classical macrophage activation pathway, the purpose of which is to destroy pathogens. Arg-I converts L-arginine to L-ornithine, which is then converted by ornithine decarboxylase to polyamines leading to cell proliferation or by ornithine aminotransferase to proline for collagen production. Cell proliferation and collagen production lead to cell growth and connective tissue formation. This arginase pathway contributes to alternative macrophage activation, the purpose of which is to repair tissue.[70] Whether a macrophage is classically activated to up regulate NOS-2 or alternatively activated to up regulate Arg-I depends on the interplay of Th1 and Th2 type cytokines. Inflammatory cytokines, such as IFN-γ, IL-12 or TNF-α will classically activate macrophages.[71] Alternatively activated macrophages may be stimulated by IL-4, IL-13, or IL-21.[71, 72] These pathways are depicted in Figure 15. The presence of the eggs themselves, and the antigens they give off, skew the immune reaction to a Th2 type response.[73-76]

Cells were challenged with the endotoxin lipopolysaccharide (LPS), and nitric oxide from the NOS-2 pathway was measured as described by the Griess assay. To study the arginase pathway, cells were plated in 6-well plates at $1x10^6$ cells/well (2 mL of $5x10^5$ cells/mL RPMI complete media) and incubated overnight. Media was then aspirated and replaced by Dulbecco's modified eagle medium (DMEM), low glucose, 1

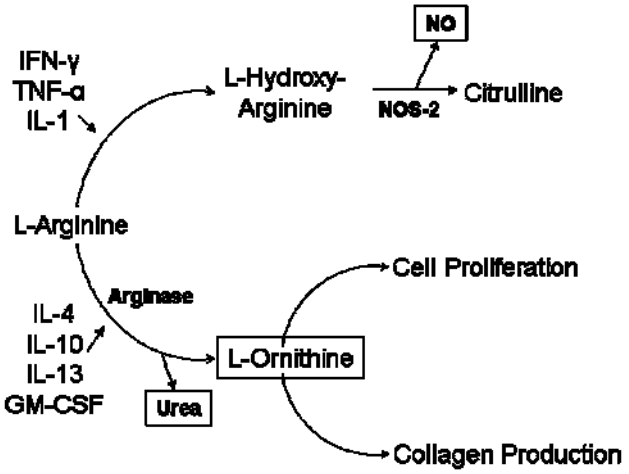

Figure 15. Th1 and Th2 stimulant response pathway in macrophage cells. Macrophages have two inducible enzymes for which arginine is the substrate: Arginase and NOS-2. Measurements were attempted of products highlighted by square borders. The top-most Th1 response was induced by LPS challenge and the bottom-most Th2 response was induced by ILs-4, 13 and 21.

g/L D-glucose, L-glutamine, 110 mg/L sodium pyruvate, 1% FBS and 1% penicillin, streptomycin. Cells were incubated 20 hours. Media was aspirated and cells were washed twice with phosphate buffered saline (PBS, without Ca^{2+}/Mg^{2+}). 2 mL DMEM without FBS was added again to each well. Cells were dosed with interleukins 4, 13 and 21 (IL-4, 13, 21) from 1-40 ng/mL, rotated by hand and incubated 48 hours. Measurements of arginase activity were attempted by monitoring the conversion of arginine to ornithine by previously described methods.[69]

Cells were harvested and lysed with lysis buffer containing 0.5% triton solution with trypsin-chymotrypsin inhibitor (0.1 mg/mL), leupeptin (0.05 mg/mL), aprotinin (0.05 mg/mL) and pheynylmethonylsulfonyl fluoride (PMSF, 0.2 mM). After lysis, 25 µL of 10 mM $MnCl_2$ was added to 25 µL of lysate from each sample. Samples were incubated at 55°C for 20 minutes. Carbonate buffer (150 µL of 0.1 M) was added to each sample. Half of the samples received 50 µL of 100 mM L-arginine, incubated at 25°C 1 hour and the reaction stopped with addition of 750 µL of glacial acetic acid. A 250 µL aliquot of 2.5 g/L ninhydrin solution (in ethanol) was added to all samples and brought to a boil for 1 hour. Ornithine production was measured at 560 nm. Significant distinction between control and experimental samples was not established due to interference with unreacted substrate. It was then that arginase activity monitoring was attempted by measurement of urea levels in preference to ornithine. This effort is outlined in appendix B.

APPENDIX B

MEASUREMENT OF ARGINASE ACTIVITY VIA UREA PRODUCTION

Another measurable product of Arginase activity is urea. An assay to detect urea based on a method by Munder et al. was developed.[77] Cells were plated and treated as described in Appendix A. In a 96 well plate 25 µL of lysate was treated with 2.5 µL of 10 mM $MnCl_2$ and heated for 10 minutes at 56˚C to activate enzyme. 25 µL of 0.5 M L-arginine, pH 9.7, substrate was then added and incubated for 120 minutes. 200 µL $H_2SO_4/H_3PO_4/H_2O$ (1/3/7, v/v/v/) was used to stop the reaction. 10 µL of 9% (w/v) α-isonitrosopropiophenone in 100% ethanol (ISPF) was added and the solution was heated at 95˚C for 30 minutes. The plate was then read at λ=540 nm. A calibration curve of urea was incorporated in the same plate and treated the same as samples. Should the calibration curve fail on any given plate, the whole plate was discarded. This assay was tried with lysate saved from previous cell experiments described in Appendix A and also with the cell treatment repeated. The urea levels produced from the cell experiments appeared to be below the detection limit of the assay.

APPENDIX C

PDTC INHBITION OF NITRIC OXIDE PRODUCTION

As an evaluation of ammonium pyrrolidine dithiocarbamate (PDTC) as a tool for probing cellular pathways, the ability of the compound to inhibit nitric oxide production in murine 264.7 macrophage-like cells was examined. Cells were plated at 500,000 cells per well to a 24 well plate and incubated overnight at 37˚C in 5% CO_2. Media was aspirated off, and cells were washed three times with PBS containing Ca^{2+} and Mg^{2+}. Cells were then treated with 500 µL media containing PDTC with concentrations varied from 0 to 100 µM, in duplicate. HNE was used as a positive control. Cells were incubated for 2 hours, then treated with 10 µL lipopolysaccharide (LPS). A Griess assay was used to assess cell response to challenge. The results are compared in Figure 16.

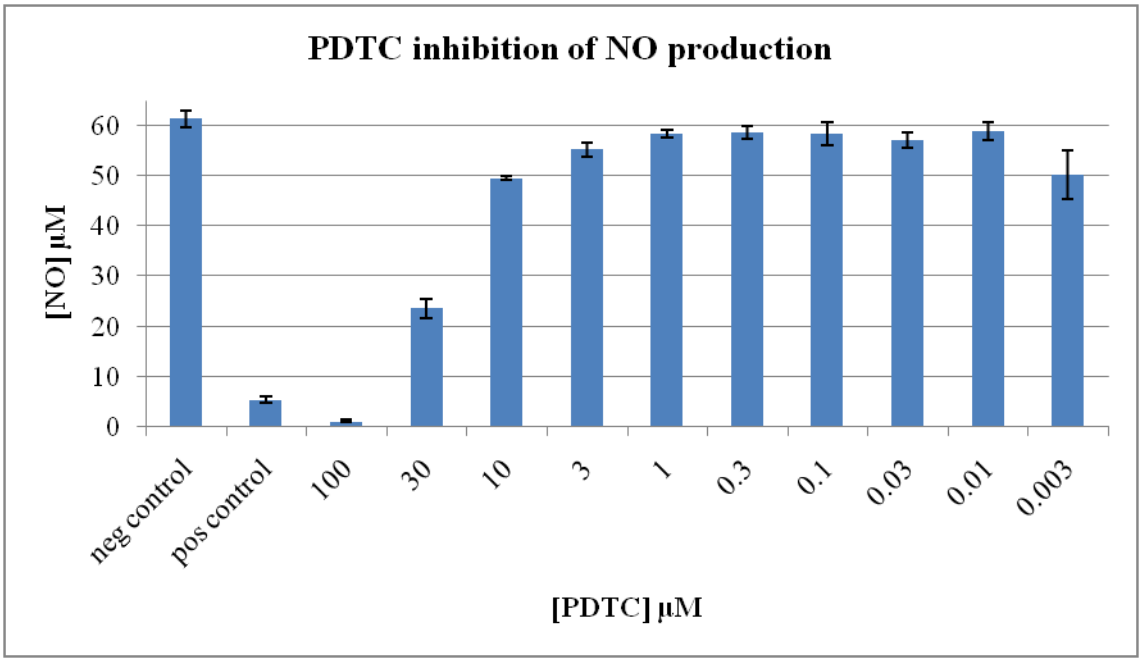

Figure 16. Calibration of PDTC inhibition of NO production in 264.7 cells.

APPENDIX D

QUANTIFICATION OF ISOKETAL FORMATION FROM ARACHIDONIC ACID AND BETA HEMATIN REACTION

In order to quantify isoK-pyridoxamine adduct from reaction of BH with AA, an isoK-4-aminomethylpyridine adduct was prepared for use as an internal standard. 4-Aminomethylpyridine (4-AMPy) is of lower molecular weight than pyridoxamine (PM), and so may be distinguished from PM via MS. 4-AMPy also has a strong affinity for isoK. The two compounds are of similar structure and elute from the described HPLC at the same time. 4-AMPy-isoK standard was prepared and cleaned by previously described methods for preparation of PM-isoK[78] by combining 25 µL of 10 mM isoK (from the lab of L. Jackson Roberts) with 20 µL of 4-AMPy in 955 µL 100 mM sodium phosphate buffer (chelexed, pH 7.4). At the same time, synthesis and cleaning of PM-isoK was set up for comparison: 25 µL of 10 mM isoK with an excess of PM in quantity sufficient 100 mM sodium phosphate to 1.000 mL. Both reactions shaken overnight at 55 rpm, 37˚C. PM-isoK and 4-AMPy-isK were cleaned on a Waters Sep-Pak C18 cartridge preconditioned with 10 mL methanol. Reaction mixtures were added to the cartridge via syringe at a flow rate of no faster than 1 mL/min. Samples were then washed at no more than 4 mL/min with 10 mL water, 10 mL methanol/water (15:85), 10 mL heptane, and 10 mL heptane/ ethyl acetate (1:1). Product was then eluted with 5 mL methanol/ ethyl acetate (1:1) at about 2 mL/min. Eluent was dried under N_2, resuspended in 400 µL of HPLC solvent A, and stored at <-20˚C until HPLC became available. HPLC solvent A was 20 mM ammonium acetated with 0.1% v/v acetic acid. Solvent B was 5 mM ammonium acetate/methanol (1:9) with 0.1% acetic acid. A Phenomenex Luna 5u C18 column was used to clean the products with the following gradient at 0.2 mL/min: 5

minutes at 100% A, ramp up to 100% B until 45 minutes, hold at 100% B until 60 minutes, gradient back to 100% A by 65 minutes, and equilibrate with 100% A until 85 minutes. Runs were monitored at λ = 320 nm, 250 nm, and 220 nm. Samples were collected in 0.5 dram glass vials and labeled with time, product and HPLC run number. Standards were then analyzed via LC-MS/MS. Tune files were created for PM-isoK with a parent ion of 501 m/z, and for 4-AMPy-isoK with a parent ion of 441 m/z. It was determined that using the column and gradient described above, both types of products eluted chiefly at 61-64 minutes.

The concentration of the 4-AMPy-isoK internal standard was approximated by UV/vis spectrometry by determining the molar absorptivity coefficient for 4-(ethylaminomethyl)pyridine. The constant was determined to be 2558.2 at 259 nm. Reactions between BH and AA were set up as described above with increasing concentrations of BH. These reactions were spiked with 4-AMPy-isoK as an internal standard and extracted with ether as described above and taken for LC-MS/MS analysis. No data was acquired due to an undiscovered leak in the column while samples were running.

APPENDIX E

COMPARISON OF HEME COMPOUNDS VIA IMMS

In order to determine if different heme species could be differentiated with ion mobility- mass spectrometry (IMMS), several species were compared, including hemin-Cl, BH and μ-oxo-[Fe(III)PPIX]. For this purpose a μ-oxo-[Fe(III)PPIX] dimer was synthesized by methods previously described.[79] Briefly, 1.00 g hemin chloride was stirred in 100 mL anhydrous methanol with 5.0 mL of 18 M H_2SO_4 overnight at room temperature. Chloroform extracts of the mixture were washed with water, saturated

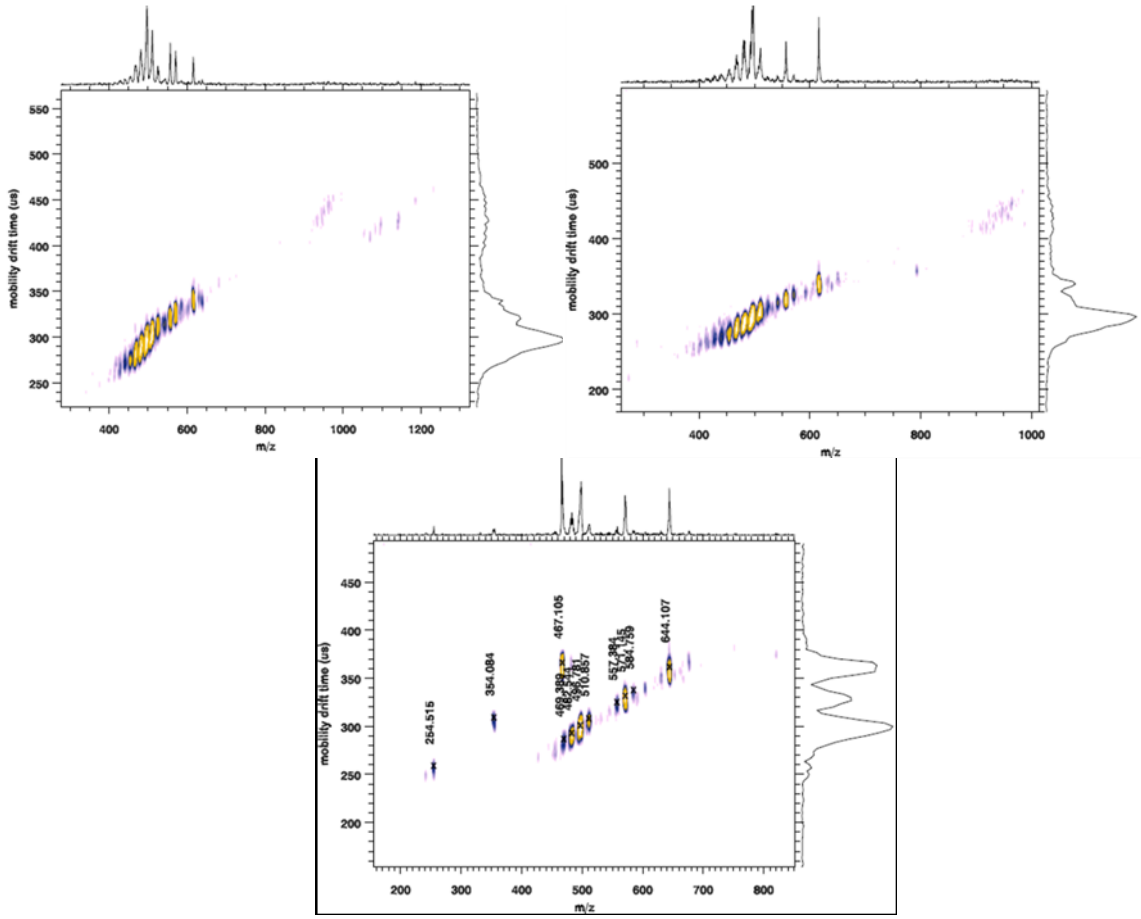

Figure 17. (a) BH with dihydroxybenzoic acid matrix. (b) hemin chloride with DHB matrix (c) with DHB matrix.

sodium bicarbonate solution (7.8 g in 100 mL), and again with water. The solution was then dried over anhydrous sodium sulfate and evaporated to dryness at reduced pressure. The product was then dissolved in benzene and chromatographed on alumina deactivated with 10% water. The major band was eluted from the column with benzene:chloroform 1:3 (v/v) and evaporated to dryness at reduced pressure. A sample was prepared at 4.7 mM in ethanol for IMMS analysis by Larissa Fenn, along with samples of 13.5 M hemin chloride and 5 mM BH. IMMS plots of these samples are compared in Figure 17.

REFERENCES

1. Hotez, P. J.; Molyneux, D. H.; Fenwick, A.; Ottesen, E.; Sachs, S. E.; Sachs, J. D., *Pl o S Medicine* **2006,** *3* (5), 576(9).
2. Chitsulo, L.; Engels, D.; Montresor, A.; Savioli, L., *Acta Tropica* **2000,** *77* (1), 41-51.
3. Roberts, L. S.; Janovy, J., Foundations of Parasitology. 2000.
4. Steinmann, P.; Keiser, J.; Bos, R.; Tanner, M.; Utzinger, J., *The Lancet Infectious Diseases* **2006,** *6* (7), 411-425.
5. Woolhouse, M. E. J., *Parasitology Today* **1998,** *14* (10), 428-434.
6. Salafsky, B.; Wang, Y. S.; Kevin, M. B.; Hill, H.; Fuscuo, A. C., *Journal of Parasitology* **1984,** *70* (4), 584-591.
7. Salafsky, B.; Wang, Y. S.; Fusco, A. C.; Antonacci, J., *Journal of Parasitology* **1984,** *70* (5), 656-660.
8. Lawrence, J. D., *The Journal of Parasitology* **1973,** *59* (1), 60-63.
9. Boros, D. L., *Clin. Microbiol. Rev.* **1989,** *2* (3), 250-269.
10. Farah, I. O.; Nyindo, M.; Suleman, M. A.; Nyaundi, J.; Kariuki, T. M.; Blanton, R. E.; Elson, L. H.; King, C. L., *Experimental Parasitology* **1997,** *86* (2), 93-101.
11. Gutteridge, J. M.; Smith, A., *Biochem. J.* **1988,** *256* (3), 861-865.
12. Halliwell, B., *Free Radical Biology and Medicine* **1989,** *7* (6), 645-651.
13. Pagola, S.; Stephens, P. W.; Bohle, D. S.; Kosar, A. D.; Madsen, S. K., *Nature* **2000,** *404* (6775), 307-310.
14. Schwarzer, E.; Arese, P., *Biochimica et Biophysica Acta (BBA) - Molecular Basis of Disease* **1996,** *1316* (3), 169-175.
15. Schwarzer, E.; Turrini, F.; Ulliers, D.; Giribaldi, G.; Ginsburg, H.; Arese, P., *Journal of Experimental Medicine* **1992,** *176* (4), 1033-1041.
16. Schwarzer, E.; Alessio, M.; Ulliers, D.; Arese, P., *Infect. Immun.* **1998,** *66* (4), 1601-1606.
17. Schwarzer, E.; Muller, O.; Arese, P.; Siems, W. G.; Grune, T., *FEBS Letters* **1996,** *388* (2,3), 119-122.
18. Omodeo-Salè, F.; Monti, D.; Olliaro, P.; Taramelli, D., *Biochemical Pharmacology* **2001,** *61* (8), 999-1009.
19. Green, M. D.; Xiao, L.; Lal, A. A., *Molecular and Biochemical Parasitology* **1996,** *83* (2), 183-188.
20. Scorza, T.; Magez, S.; Brys, L.; De Baetselier, P., *Parasite Immunology* **1999,** *21* (11), 545-554.
21. Pichyangkul, S.; Saengkrai, P.; Webster, H. K., *Am J Trop Med Hyg* **1994,** *51* (4), 430-435.
22. Taramelli, D.; Basilico, N.; Pagani, E.; Grande, R.; Monti, D.; Ghione, M.; Olliaro, P., *Experimental Parasitology* **1995,** *81* (4), 501-511.
23. Taramelli, D.; Recalcati, S.; Basilico, N.; Olliaro, P.; Cairo, G., *Lab Invest* **2000,** *80* (12), 1781-1788.
24. Oliveira, M. F.; Timm, B. L.; Machado, E. A.; Miranda, K.; Attias, M.; Silva, J. R.; Dansa-Petretski, M.; de Oliveira, M. A.; de Souza, W.; Pinhal, N. M.; Sousa, J. J. F.; Vugman, N. V.; Oliveira, P. L., *FEBS Letters* **2002,** *512* (1-3), 139-144.

25. Fitch, C. D.; Kanjananggulpan, P., *Journal of Biological Chemistry* **1987,** *262* (32), 15552-15555.
26. Slater, A. F.; Swiggard, W. J.; Orton, B. R.; Flitter, W. D.; Goldberg, D. E.; Cerami, A.; Henderson, G. B., *Proceedings of the National Academy of Sciences of the United States of America* **1991,** *88* (2), 325-329.
27. Bohle, D. S.; Dinnebier, R. E.; Madsen, S. K.; Stephens, P. W., *J. Biol. Chem.* **1997,** *272* (2), 713-716.
28. Yamada, K. A.; Sherman, I. W., *Experimental Parasitology* **1979,** *48* (1), 61-74.
29. Goldie, P.; Roth, E. F., Jr.; Oppenheim, J.; Vanderberg, J. P., *Am J Trop Med Hyg* **1990,** *43* (6), 584-596.
30. Bohle, D. S.; Helms, J. B., *Biochemical and Biophysical Research Communications* **1993,** *193* (2), 504-508.
31. Schwarzer, E.; Kuhn, H.; Valente, E.; Arese, P., *Blood* **2003,** *101* (2), 722-728.
32. Schwarzer, E.; Turrini, F.; Giribaldi, G.; Cappadoro, M.; Arese, P., *Biochimica et Biophysica Acta (BBA) - Molecular Basis of Disease* **1993,** *1181* (1), 51-54.
33. Turrini, F.; Schwarzer, E.; Arese, P., *Parasitology Today* **1993,** *9* (8), 297-300.
34. Brown, A. E.; Webster, H. K.; Teja-Isavadharm, P.; Keeratithakul, D., *Clinical and Experimental Immunology* **1990,** *82* (1), 97-101.
35. Levesque, M. A.; Sullivan, A. D.; Meshnick, S. R., *The Journal of Parasitology* **1999,** *85* (3), 570-573.
36. Fiori, P. L.; Rappelli, P.; Mirkarimi, S. N.; Ginsburg, H.; Cappuccinelli, P.; Turrini, F., *Parasite Immunology* **1993,** *15* (12), 647-655.
37. Prada, J.; Malinowski, J.; Muller, S.; Bienzle, U.; Kremsner, P. G., *Am J Trop Med Hyg* **1996,** *54* (6), 620-624.
38. Millington, O.; Di Lorenzo, C.; Phillips, R.; Garside, P.; Brewer, J., *Journal of Biology* **2006,** *5* (2), 5.
39. Urban, B.; Todryk, S., *Journal of Biology* **2006,** *5* (2), 4.
40. Carney, C. K.; Schrimpe, A. C.; Halpenny, K.; Harry, R. S.; Miller, C. M.; Broncel, M.; Sewell, S. L.; Schaff, J. E.; Deol, R.; Carter, M. D.; Wright, D. W., *JBIC* **2006,** *11* (7), 917-929.
41. Wynn, T. A.; Thompson, R. W.; Cheever, A. W.; Mentink-Kane, M. M., *Immunological Reviews* **2004,** *201* (1), 156-167.
42. Wilson, M. S.; Mentink-Kane, M. M.; Pesce, J. T.; Ramalingam, T. R.; Thompson, R.; Wynn, T. A., *Immunol Cell Biol* **2006,** *85* (2), 148-154.
43. Kaplan, M. H.; Whitfield, J. R.; Boros, D. L.; Grusby, M. J., *J Immunol* **1998,** *160* (4), 1850-1856.
44. Pearce, E. J.; MacDonald, A. S., *Nat Rev Immunol* **2002,** *2* (7), 499-511.
45. Cheever, A. W.; Williams, M. E.; Wynn, T. A.; Finkelman, F. D.; Seder, R. A.; Cox, T. M.; Hieny, S.; Caspar, P.; Sher, A., *J Immunol* **1994,** *153* (2), 753-759.
46. Reiman, R. M.; Thompson, R. W.; Feng, C. G.; Hari, D.; Knight, R.; Cheever, A. W.; Rosenberg, H. F.; Wynn, T. A., *Infect. Immun.* **2006,** *74* (3), 1471-1479.
47. Stenger, R. J.; Warren, K. S.; Johnson, E. A., *Experimental and Molecular Pathology* **1967,** *7* (1), 116-132.
48. Phillips, S. M.; DiConza, J. J.; Gold, J. A.; Reid, W. A., *J Immunol* **1977,** *118* (2), 594-599.

49. Hanna, S.; Gharib, B.; Lepidi, H.; Montet, J.-C.; Dumon, H.; de Reggi, M., *Parasitology Research* **2005,** *96* (1), 6-11.
50. Abdallahi, O. M. S.; Hanna, S.; Reggi, M.; Gharib, B., *Liver* **1999,** *19* (6), 495-500.
51. Gharib, B.; Abdallahi, O. M. S.; Dessein, H. l.; Reggi, M. D., *Journal of hepatology* **1999,** *30* (4), 594-602.
52. Carter, M. D.; Reese Harry, S.; Wright, D. W., *Biochemical and Biophysical Research Communications* **2007,** *363* (3), 867-872.
53. Oliveira, M. F.; d'Avila, J. C. P.; Torres, C. R.; Oliveira, P. L.; Tempone, A. J.; Rumjanek, F. D.; Braga, C. M. S.; Silva, J. R.; Dansa-Petretski, M.; Oliveira, M. A.; de Souza, W.; Ferreira, S. T., *Molecular and Biochemical Parasitology* **2000,** *111* (1), 217-221.
54. Pandey, A. V.; Tekwani, B. L.; Pandey, V. C., *Biomedical Research* **1995,** *16* (2), 115-120.
55. Deegan, T.; Maegraith, B., *Ann Trop Med Parasitol* **1956,** *50* (2), 194-211.
56. Deegan, T.; Maegraith, B., *Ann Trop Med Parasitol* **1956,** *50* (2), 212-222.
57. Sullivan, D. J.; Gluzman, I. Y.; Russell, D. G.; Goldberg, D. E., *Proceedings of the National Academy of Sciences of the United States of America* **1996,** *93* (21), 11865-11870.
58. Oliveira, M. F.; Kycia, S. W.; Gomez, A.; Kosar, A. J.; Bohle, D. S.; Hempelmann, E.; Menezes, D.; Vannier-Santos, M. A.; Oliveira, P. L.; Ferreira, S. T., *FEBS Letters* **2005,** *579* (27), 6010-6016.
59. Noland, G. S.; Briones, N.; Sullivan, D. J., *Molecular and Biochemical Parasitology* **2003,** *130* (2), 91-99.
60. Brown, W. D.; Harris, L. S.; Olcott, H. S., *Archives of Biochemistry and Biophysics* **1963,** *101*, 14-20.
61. Davies, S. S.; Brantley, E. J.; Voziyan, P. A.; Amarnath, V.; Zagol-Ikapitte, I.; Boutaud, O.; Hudson, B. G.; Oates, J. A.; Roberts, L. J., *Biochemistry* **2006,** *45* (51), 15756-15767.
62. Amarnath, V.; Amarnath, K.; Amarnath, K.; Davies, S.; Roberts, L. J., *Chemical Research in Toxicology* **2004,** *17* (3), 410-415.
63. Kubata, B. K.; Eguchi, N.; Urade, Y.; Yamashita, K.; Mitamura, T.; Tai, K.; Hayaishi, O.; Horii, T., *J. Exp. Med.* **1998,** *188* (6), 1197-1202.
64. El-Sokkary, G. H.; Omar, H. M.; Hassanein, A.-F. M. M.; Cuzzocrea, S.; Reiter, R. J., *Free Radical Biology and Medicine* **2002,** *32* (4), 319-332.
65. Esterbauer, H.; Schaur, R. J.; Zollner, H., *Free Radical Biology and Medicine* **1991,** *11* (1), 81-128.
66. Bedossa, P.; Houglum, K.; Trautwein, C.; Holstege, A.; Chojkier, M., *Hepatology* **1994,** *19* (5), 1262-1271.
67. Konarska, L.; Tomaszewski, L., *Clinica Chimica Acta* **1986,** *154*, 7-18.
68. Chinard, F. P., *Journal of Biological Chemistry* **1952,** *199*, 91-95.
69. Chinard, F. P., *J. Biol. Chem.* **1952,** *199* (1), 91-95.
70. Stein, M.; Keshav, S.; Harris, N.; Gordon, S., *J. Exp. Med.* **1992,** *176* (1), 287-292.
71. Gordon, S., *Nat Rev Immunol* **2003,** *3* (1), 23-35.

72. Pesce, J.; Kaviratne, M.; Ramalingam, T. R.; Thompson, R. W.; Urban, J. F.; Cheever, A. W.; Young, D. A.; Collins, M.; Grusby, M. J.; Wynn, T. A., *Journal of Clinical Investigation* **2006,** *116* (7), 2044-2055.
73. Faveeuw, C.; Angeli, V.; Fontaine, J.; Maliszewski, C.; Capron, A.; Van Kaer, L.; Moser, M.; Capron, M.; Trottein, F., *J Immunol* **2002,** *169* (2), 906-912.
74. Wynn, T. A.; Eltoum, I.; Cheever, A. W.; Lewis, F. A.; Gause, W. C.; Sher, A., *J Immunol* **1993,** *151* (3), 1430-1440.
75. Chensue, S. W.; Terebuh, P. D.; Warmington, K. S.; Hershey, S. D.; Evanoff, H. L.; Kunkel, S. L.; Higashi, G. I., *J Immunol* **1992,** *148* (3), 900-906.
76. Pearce, E. J.; Caspar, P.; Grzych, J. M.; Lewis, F. A.; Sher, A., *J. Exp. Med.* **1991,** *173* (1), 159-166.
77. Munder, M.; Eichmann, K.; Modolell, M., *The Journal of Immunology* **1998,** *160* (11), 5347-5354.
78. Davies, S. S.; Amarnath, V.; Brame, C. J.; Boutaud, O.; Roberts, L. J., *Nat. Protocols* **2007,** *2* (9), 2079-2091.
79. O'Keeffe, D. H.; Barlow, C. H.; Smythe, G. A.; Fuchsman, W. H.; Moss, T. H.; Lilienthal, H. R.; Caughey, W. S., *Bioinorganic Chemistry* **1975,** *5* (2), 125-147.